Noninvasive evaluation of hepatic fibrosis using acoustic radiation force-based shear stiffness in patients with nonalcoholic fatty liver disease

Mark L. Palmeri[1,*], Michael H. Wang[1], Ned C. Rouze[1], Manal F. Abdelmalek[2], Cynthia D. Guy[3], Barry Moser[4], Anna Mae Diehl[2], Kathryn R. Nightingale[1]

[1]Department of Biomedical Engineering, Duke University, Durham, NC, USA; [2]Division of Gastroenterology and Hepatology, Duke University Medical Center, Durham, NC, USA; [3]Department of Pathology, Duke University Medical Center, Durham, NC, USA; [4]Department of Biostatistics and Bioinformatics, Duke University Medical Center, Durham, NC, USA

Background & Aims: Nonalcoholic fatty liver disease (NAFLD), the most common form of chronic liver disease in developed countries, may progress to nonalcoholic steatohepatitis (NASH) in a minority of people. Those with NASH are at increased risk for cirrhosis and hepatocellular carcinoma. The potential risk and economic burden of utilizing liver biopsy to stage NAFLD in an overwhelmingly large at-risk population are enormous; thus, the discovery of sensitive, inexpensive, and reliable non-invasive diagnostic modalities is essential for population-based screening.

Methods: Acoustic Radiation Force Impulse (ARFI) shear wave imaging, a noninvasive method of assessing tissue stiffness, was used to evaluate liver fibrosis in 172 patients diagnosed with NAFLD. Liver shear stiffness measures in three different imaging locations were reconstructed and compared to the histologic features of NAFLD and AST-to-platelet ratio indices (APRI).

Results: Reconstructed shear stiffnesses were not associated with ballooned hepatocytes ($p = 0.11$), inflammation ($p = 0.69$), nor imaging location ($p = 0.11$). Using a predictive shear stiffness threshold of 4.24 kPa, shear stiffness distinguished low (fibrosis stage 0–2) from high (fibrosis stage 3–4) fibrosis stages with a sensitivity of 90% and a specificity of 90% (AUC of 0.90). Shear stiffness had a mild correlation with APRI ($R^2 = 0.22$). BMI >40 kg/m^2 was not a limiting factor for ARFI imaging, and no correlation was noted between BMI and shear stiffness ($R^2 = 0.05$).

Conclusions: ARFI imaging is a promising imaging modality for assessing the presence or absence of advanced fibrosis in patients with obesity-related liver disease.

Introduction

Nonalcoholic fatty liver disease (NAFLD), a serious public health concern, is increasing with the rise in obesity and is currently the most common form of chronic liver disease in both children and adults [1,2]. Estimates suggest that approximately 80 million Americans may have NAFLD [3]. NAFLD is a clinicopathologic condition associated with over-accumulation of fat in the liver; it is characterized by simple steatosis on the benign end of the spectrum with progression to nonalcoholic steatohepatitis (NASH), an intermediate stage of the disease, and increased risk for progression to cirrhosis, need for liver transplant and/or hepatocellular carcinoma in a minority of patients with NAFLD [4–6]. The clinician has limited ability to characterize disease severity by patient history, physical examination, routine laboratory studies, and/or radiological imaging modalities [6]. Liver biopsy remains the only reliable "gold standard" method for distinguishing benign steatosis from NASH and staging the severity of hepatic fibrosis for patients with obesity-related liver disease [7]. However, due to increased cost, possible risk, and health-care resource utilization, an invasive liver biopsy is poorly suited as a diagnostic test for such a prevalent condition. Furthermore, the histologic lesions of NASH are unevenly distributed throughout the liver parenchyma; therefore, sampling error of liver biopsy can result in substantial stratification and staging inaccuracies [8].

Ultrasound is an ideal technology to non-invasively characterize advanced liver diseases. The majority of the liver can be interrogated using a variety of imaging locations (i.e., both inter- and subcostally). Further, ultrasound equipment and scanners have become much more compact, are portable, can be utilized in a variety of clinical settings (inpatient and outpatient, clinical and radiology suites), and can be performed at the bedside as diagnostic tools or for assessment of anatomy at the time of liver biopsy.

The use of ultrasound to characterize liver stiffness has been explored with transient elastography (FibroScan®, EchoSens,

Paris, France), which has been shown to represent a promising non invasive tool for staging hepatic fibrosis [9,18]. While body mass indices (BMI) >28 kg/m^2 have been identified as an independent risk factor for failure to obtain a measure of liver elastography [10], more recent clinical studies using the FibroScan® system have appeared in the literature that have demonstrated increasing liver stiffness with advanced fibrosis in patients with NAFLD [11–13]. Patients with ascites, however, present challenges for systems such as the FibroScan® since shear waves will not propagate through fluids, making shear stiffness reconstructions in these patients impossible with transient elastography; this is not a limitation for the Acoustic Radiation Force Impulse (ARFI) shear wave imaging technique presented herein [14,15]. Transient tissue deformations of several microns are induced in liver tissue by acoustic radiation force, generating shear waves that can be used to estimate the tissue stiffness, as detailed in [15].

Given NAFLD's enormous public health burden, there is a great need for the development and optimization of a non-invasive approach to determine the presence or absence of advanced liver disease. We evaluated ARFI shear wave imaging as a potential non-invasive method to assess the hepatic fibrosis stage in patients with biopsy-proven NAFLD.

Patients and methods

Study design and population

We performed a retrospective/prospective study of patients with biopsy-proven NAFLD at the Duke University Medical Center. Patients were enrolled from March 2008 to March 2010. Patients who met the following criteria were used for our analysis ($n = 172$): (1) age 18 or older; (2) available liver histology data; (3) no significant alcohol consumption (<14 drinks/week in men or <7 drinks/week in women on average within the past 2 years); (4) no other coexisting causes of chronic liver disease as determined by a hepatologist. This study was approved

Table 1. Study subject demographics.

	Totals	Successful Stiffness Reconstruction	Unsuccessful Stiffness Reconstruction
Study Subjects	172	135	37
Gender			
Male	65	51	14
Female	107	84	23
Body Mass Index			
<18	1	1	0
18 - 23	8	8	0
23 - 30	45	39	6
30 - 40	85	68	17
>40	33	19	14
Fibrosis Stage			
0	31	26	5
1	39	34	5
2	46	35	11
3	36	22	14
4	20	18	2

by the Institutional Review Board at the Duke University, and each study subject provided written informed consent prior to enrollment in the study. Table 1 shows a summary of the study subject enrollment metrics.
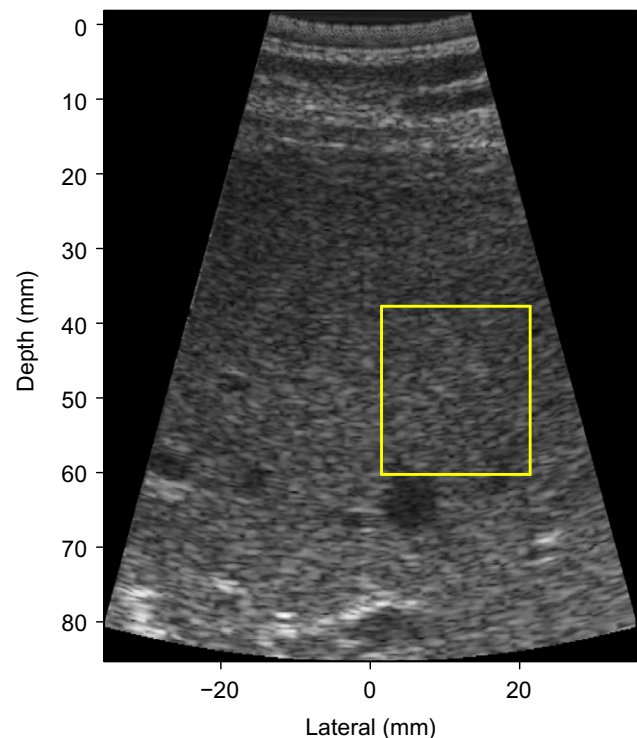
Data acquisition and processing

Shear wave data acquisition and processing was performed as previously reported in earlier technical publications using a customized Siemens SONOLINE Antares™ scanner and a CH41 transducer (Siemens Healthcare, Ultrasound Business Unit, Mountain View, CA) [15,19]. Five different people performed the imaging during this study, each of whom had training scanning volunteers before scanning study subjects to reduce operator variability; inter-operator variability was not analyzed in this study. All patients ($n = 172$) undergoing a percutaneous liver biopsy for the diagnosis and staging of presumed NALFD were imaged within minutes prior to liver biopsy. Shear stiffnesses were characterized in three different locations of the liver: (1) superior intercostal (i.e., 9–10th rib intercostals space coinciding most often with the location of the liver biopsy needle insertion), (2) inferior intercostal (i.e., 10–11th rib intercostals space, typically 1–2 ribs spaces inferior to the superior location), and (3) lateral subcostal. Three replicate shear stiffness data acquisitions were performed at each imaging location for a total of nine data acquisitions per patient.

Study subjects were asked to suspend breathing for each of the nine data acquisitions, which lasted approximately 5 s. After the study subject paused their breathing, an imaging location was found that had homogeneous liver parenchyma on standard B-mode imaging, devoid of any vessels or other substructures of the liver; an example of such a region of interest (ROI) is shown in Fig. 1. Data were acquired once a suitable location was found during imaging. The patient was then instructed to resume breathing after the shear wave data were saved.

The RANSAC algorithm described by Wang *et al.* was used for all of the shear wave speed estimates presented herein [19]. Quantitative criteria were used to eliminate spurious estimates corrupted by excessive motion artifact, poor signal-to-noise ratio (SNR), and inadequate imaging windows [19]. Patients who

Fig. 1. B-mode image from one of the NAFLD study subjects. The yellow box represents the ROI for reconstructing the shear stiffness, which is chosen to be free of vessels and other liver substructures. The radiation force excitation was applied at a lateral position of 0, and propagation was monitored to the right (positive lateral locations).

Genetic and Metabolic Diseases

Research Article

had an IQR/mean >0.3 after outlier rejection were considered too variable and not successfully reconstructed. Shear wave speed estimates (c_T) were converted to shear stiffnesses (μ) using the expression:

$$\mu = c_T^2 \rho \tag{1}$$

where ρ represents the constant density (1.0 g/cm^3) in the assumed linear, isotropic elastic liver tissue [15]. Some literature using the commercial implementation of this technique (VirtualTouch™ Tissue Quantification on the Siemens ACUSON S2000) may report shear wave speeds (c_T) instead of shear moduli; the quoted shear moduli (μ) in this paper (in kPa) can be converted to shear wave speeds (c_T, in m/s) using the relationship $c_T = \mathrm{sqrt}(\mu)$ (Eq. (1)). Literature involving the FibroScan® quote liver stiffnesses as Young's moduli (E) instead of shear moduli; under the assumption of tissue incompressibility that is made in this setting, shear and Young's moduli can be converted using the expression $E = 3\mu$.

Liver histology

The primary outcome in this study was liver histology in patients with NAFLD. All liver biopsy specimens were stained with hematoxylin-and-eosin and Masson's trichrome stains. Liver histology was reviewed and scored by a liver histopathologist (CG) according to the published NASH Clinical Research Network scoring system [22]. The following histologic features of NAFLD were evaluated in this study: the grades of lobular inflammation, and ballooning, and the stage of fibrosis. Briefly, lobular inflammation was graded into 0–3 based on the numbers of inflammatory foci per 20× field: 0 (grade 0), <2 (grade 1), 2–4 (grade 2), and >4 (grade 3). Ballooning was graded into 0–2: none (grade 0), few (grade 1), or many (grade 2). Fibrosis was classified into five stages: none, normal connective tissue (stage 0); zone 3 perisinusoidal or periportal fibrosis (stage 1; 1a = mild, zone 3, perisinusoidal, 1b = moderate, zone 3, perisinusoidal, 1c = portal/periportal); moderate, zone 3; perisinusoidal and portal/periportal fibrosis (stage 2); bridging fibrosis (stage 3); and cirrhosis (stage 4). For the purpose of these analyses, fibrosis stages 1a, 1b, and 1c were combined and treated as stage 1.

AST to platelet ratio index (APRI)

The aspartate aminotransferase to platelet ratio index (APRI) has been recognized as a noninvasive test to characterize the degree of liver fibrosis in the setting of NAFLD [20]. APRI was calculated for all study subjects as follows [21]:

$$\mathrm{APRI} = [(\mathrm{AST/ULN})]/(\mathrm{Platelet\ count}) * 100, \tag{2}$$

where ULN represents the AST upper level of normal (56 IU/L) and the platelet count has units of 10^9/L.

Statistical analysis

The shear stiffness data from the three imaging locations were analyzed to (1) evaluate the stiffness variability between replicate measures in the same patient and the same location, (2) evaluate the stiffness variability between different locations in the same patient, and (3) evaluate the stiffness variability averaged over replicate measures and locations as a function of fibrosis stage. A log transformation was applied to reduce the heterogeneity in the variances across fibrosis stage; the SAS (SAS Institute, Inc., Cary, NC) PROC MIXED, and PROC VARCOMP procedures were used for statistical testing. Significance was determined at an overall Bonferroni 0.10 level.
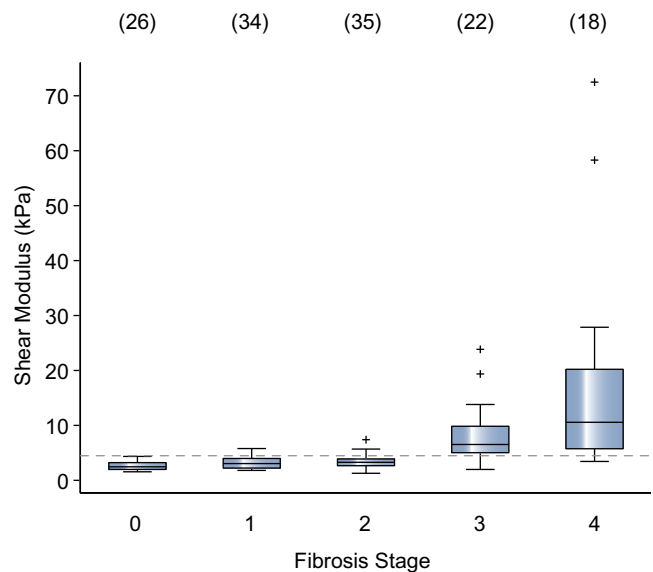
Results

One hundred thirty five of the 172 total subjects had successful shear stiffness reconstruction using the RANSAC algorithm. Table 1 outlines the distribution of study subjects as a function of gender, BMI, and fibrosis stage. Liver stiffness did not vary significantly as a function of imaging location ($p = 0.11$); therefore, the stiffness values from all imaging locations were pooled together for each study subject. The IQR/mean shear stiffness over all successfully reconstructed patients was 0.19 ± 0.13, allowing us to use the mean stiffness as a representative quantity
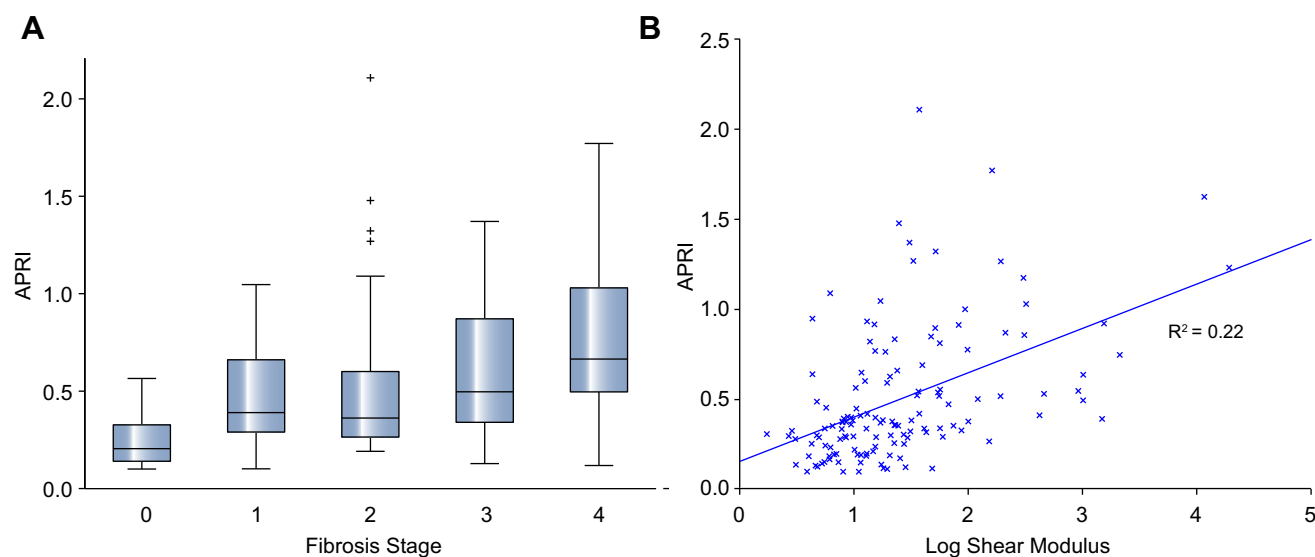
for each patient. Fig. 2 shows the mean reconstructed shear moduli from these 135 successfully-reconstructed study subjects as a function of their biopsy-determined fibrosis stage. Fibrosis stages 0–2 are significantly different from fibrosis stages 3–4 ($p < 0.0001$); based on these data, we can calculate a simple threshold of liver shear stiffness to distinguish these two groups of fibrosis as the mean log stiffness between the F2 and F3 populations. Using this calculated shear stiffness threshold of $\geqslant 4.24$ kPa (as indicated in the horizontal dashed line in Fig. 2), ARFI shear wave imaging yields a sensitivity of 90% and a specificity of 90% with an AUC value of 0.90.

The APRI is a convenient, noninvasive, blood-marker-based metric to evaluate the presence of advanced fibrosis in NAFLD patients. As expected, Fig. 3A shows the increase in APRI as a function of fibrosis stage. There is moderate correlation between APRI and mean liver shear stiffness, as shown in Fig. 3B ($R^2 = 0.22$, $p < 0.001$).
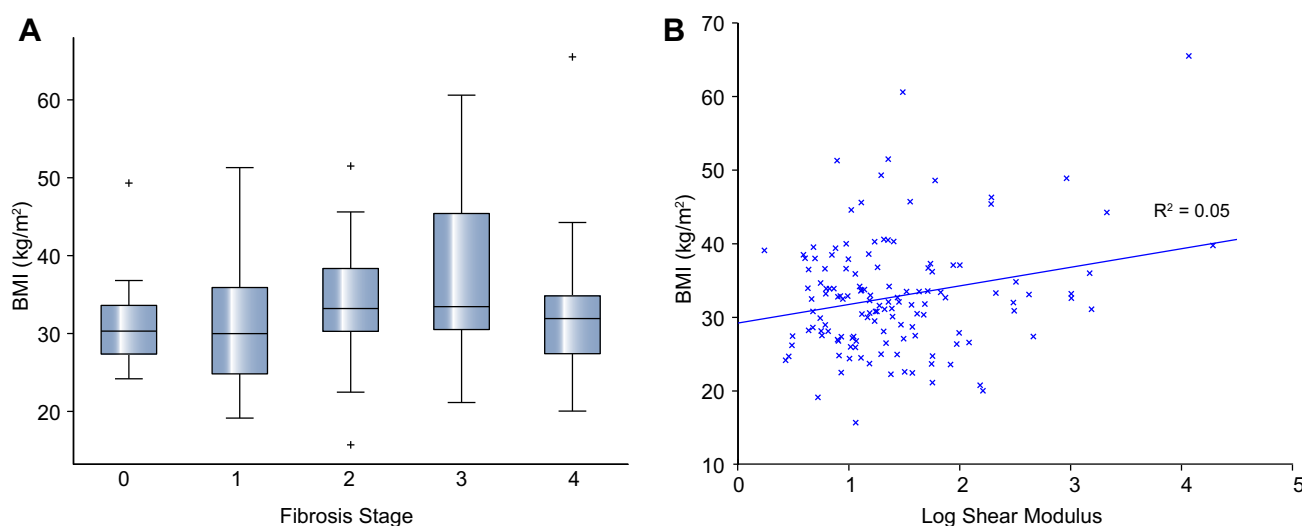
Fig. 4 shows the mean reconstructed shear moduli in the study subjects as a function of their BMI. There is no significant correlation between patient BMI and fibrosis stage (Fig. 4A) or liver stiffness (Fig. 4B, $R^2 = 0.05$, $p < 0.01$). The overall BMI distribution of patients in this study is shown in Fig. 5, with the portion of subjects with successful shear stiffness reconstructions indicated in gray (represented with percentages in text above each bar). The percentage of patients with successful shear stiffness reconstructions does decrease with increasing BMI, with 100% yield for BMI <23 kg/m^2 and 58% yield for BMI >40 kg/m^2, including successful stiffness reconstruction in a patient with a BMI = 66 kg/m^2 (Figs. 4A and 5). One of these patients presented with ascites that were visualized during the ultrasound exam;

Fig. 2. Reconstructed shear moduli in 135 patients being evaluated for NAFLD as a function of their biopsy-proven fibrosis stage. The boxes represent the interquartile range (IQR), while the whiskers represent 1.5 times the respective IQR level over the mean stiffnesses for each study subject (the mean of three replicate measures in the three imaging locations with an IQR/mean <0.3). The number of study subjects for each fibrosis stage is indicated in parentheses. The horizontal dashed line represents the threshold (4.24 kPa) to distinguish fibrosis stages F0–2 from F3–4.

A

B

Fig. 3. APRI as a function of fibrosis score and liver shear stiffness. (A) APRI as a function of fibrosis score; (B) APRI as a function of reconstructed log shear stiffness ($R^2 = 0.22$, p <0.001).

A

B

Fig. 4. BMI as a function of fibrosis score and liver shear stiffness. (A) BMI as a function of fibrosis score; (B) mean reconstructed log shear stiffness for each study subject as a function of study subject BMI. No correlation between mean liver stiffness and BMI was noted ($R^2 = 0.05$, p <0.01).

shear stiffness reconstructions ($\mu = 12.0 \pm 2.2$ kPa) successfully predicted this patient as being cirrhotic (F4).
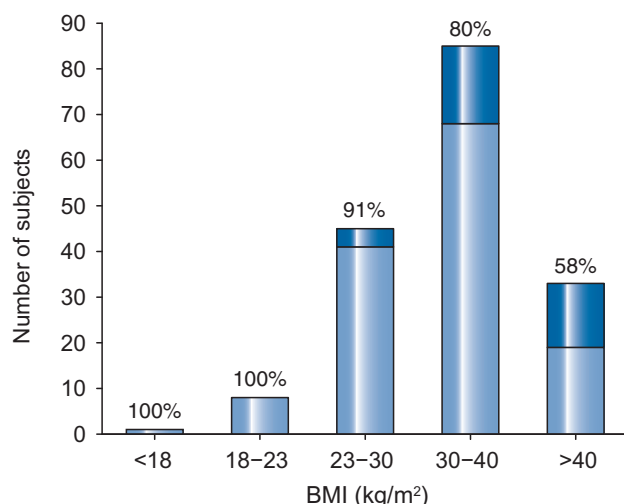
The effects of hepatocyte ballooning (Fig. 6) and inflammation (Fig. 7) were also tested for their effect on the shear stiffness measurements. Neither variable was found to be significant at the 0.1 level, with $p = 0.11$ for the ballooning and $p = 0.69$ for the inflammation.
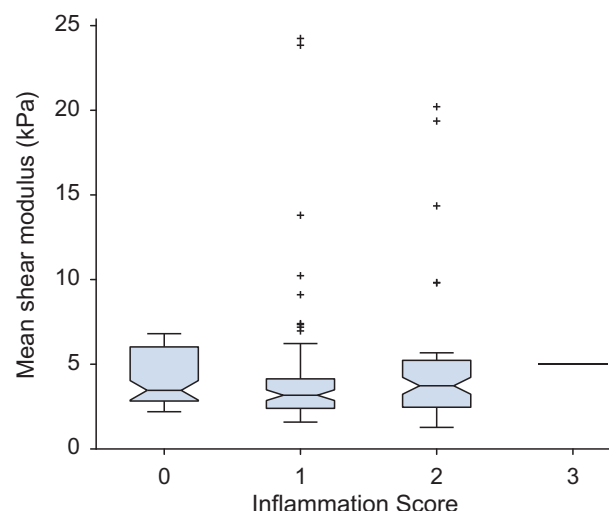
Discussion

ARFI shear wave imaging was able to successfully reconstruct liver stiffnesses in patients with fibrosis stages ranging from F0 to F4, with the most significant distinction occurring between patients grouped with little-to-moderate fibrosis (F0–2) versus those with advanced fibrosis/cirrhosis (F3–4). These results are consistent with those presented by Wong *et al.* [12] with the FibroScan®, though Yonega *et al.* did show more separation between the little-to-moderate fibrosis stages [11]. Both Yoneda *et al.* and Wong *et al.* showed increasing variability in the liver stiffness with increasing fibrosis, which is consistent with our results (Fig. 2). Wong *et al.* went onto establish stiffness thresholds to distinguish F3–4 fibrosis from less severe fibrosis, with a shear stiffness of 2.9 kPa providing sensitivity and specificity values of ~83% [12]. Applying a shear stiffness threshold of 4.2 kPa to our data yielded a sensitivity and specificity of ~90%.
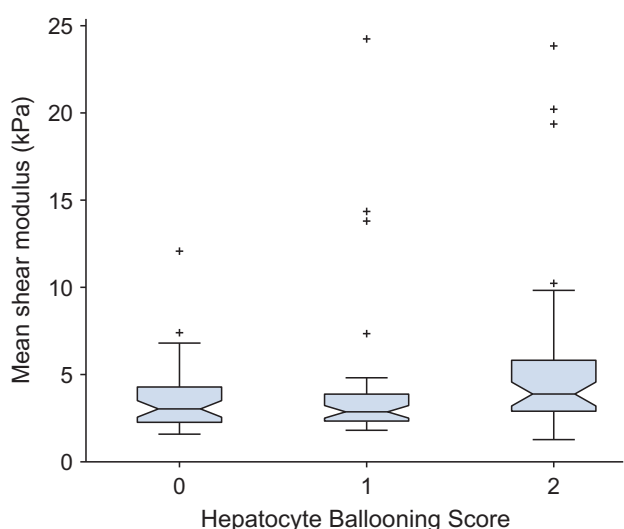
Research Article

Fig. 5. Distribution of study subject BMIs. Successful shear stiffness reconstructions are indicated in light blue, while unsuccessful shear stiffness reconstructions are indicated in dark blue. The percentages above each bar represent the percentage of successful reconstructions.

Fig. 7. Box plots of mean reconstructed shear stiffness for different biopsy-proven inflammation scores. No significant trends in shear stiffness exist as a function of inflammation ($p = 0.69$).

Fig. 6. Box plots of mean reconstructed shear stiffness for different biopsy-proven hepatocyte ballooning score. No significant trends in shear stiffness exist as a function of hepatocyte ballooning ($p = 0.11$).

While both studies demonstrate similar trends, the difference in absolute threshold value is likely due to differences in the characteristics of the mechanical excitation [32]. Future, larger scale studies need to be performed to validate the predictive value of these stiffness metrics and to study the dispersive mechanical properties of the liver.

The primary role of liver biopsy in the evaluation of NAFLD is the exclusion of advanced fibrosis and/or cirrhosis as the presence of such would alter clinical management and follow-up. The ability to use ARFI imaging as a non-invasive screening test to discern those patients with advanced liver disease could spare patients the potential complications of a liver biopsy, reduce associated health care costs and resource utilization, and allow adequate screening of advanced liver disease to be applied to a larger population of at risk patients.

Acoustic radiation force-based shear stiffness reconstruction techniques have started to appear on commercial scanners that are being used in clinical studies of liver fibrosis due to a variety of etiologies [17,25,30,31]. Lupsor *et al.* [26] and Friedrich-Rust *et al.* [27] utilized the Virtual Touch™ Tissue Quantification mode on the Siemens ACUSON S2000 scanner (a commercial implementation of the acoustic radiation force technologies presented in this manuscript) to study the correlation between shear stiffness values (measured directly as shear wave speeds) with liver fibrosis in viral hepatitis patients; they found very similar trends compared to those found in the NAFLD patient population in this study. Yoneda *et al.* also recently compared transient elastography (i.e., the FibroScan® system) with Virtual Touch™ Tissue Quantification in NAFLD patients and found a good correlation between the two systems ($R^2 = 0.56$, $p < 0.0001$) [13]. However, it should be noted that this Japanese study population tended to be leaner (BMI 27 ± 4.7 kg/m^2) with few patients with advanced fibrosis or cirrhosis (F3, $n = 4$; F4, $n = 6$). This is in contrast to our study with over 60% of NAFLD patients having BMI >30 kg/m^2 and a large cohort of patients with biopsy-proven advanced fibrosis/cirrhosis (F3–4, $n = 40$), confirming that shear stiffness reconstruction is possible in the majority of obese and even severely obese patients with NAFLD, as is typically observed in Western countries. Overall, the results from these ultrasound-based elasticity measurement systems are in good agreement with those found in the Magnetic Resonance Elastography (MRE) literature [28,29]. Multi-center, prospective studies need to be performed to rigorously evaluate the clinical utility of ARFI shear wave imaging, in comparison with tools such as the FibroScan®, as a function of controlled patient population variables, including gender, age, BMI, and liver disease etiology.

The shear stiffness reconstructions did not significantly differ based on the imaging location, which allowed all of the analysis presented herein to be performed using mean shear stiffness values for each study subject. Liver shear stiffness was also not significantly affected by the degree of hepatocyte ballooning (Fig. 6), nor the amount of hepatic inflammation (Fig. 7). One other factor that has been reported to have an effect on liver stiffness is hepatic congestion, which can increase liver stiffness [23,24]. However, no patients with known right-sided heart failure were included in this study, and no signs of sinusoidal dilation were noted on liver biopsy, thus reducing the likelihood that this factor would confound our interpretation of the study results. The APRI trends with liver fibrosis shown in Fig. 3A are consistent with those reported by Loaeza-del-Castillo *et al.* [20], and shear stiffness demonstrated a mild correlation with APRI (Fig. 3A).

There was no correlation between BMI and liver stiffness, and stiffness values were successfully reconstructed in subjects with BMIs up to 66 kg/m^2 (the highest BMI in this study). However, 37 patients did not yield successful liver shear stiffness estimates; of these patients, many of them had high BMIs (>40 kg/m^2) (Fig. 5). One likely explanation for this trend is the increasing amount of adipose tissue between the skin and the liver capsule that can occur in subjects with higher BMIs. The magnitude of the applied radiation force in ARFI imaging decreases when more acoustic energy is absorbed by the intervening tissue along the acoustic propagation path. Subcutaneous adipose tissue can have considerably higher ultrasonic loss (attenuation) than liver tissue. Therefore, patients with high BMI, who often have several centimeters of subcutaneous adipose tissue, may be more likely to experience smaller applied radiation forces, which can lead to poor data SNR and a failure to yield a stiffness estimate [15,19]. This additional adipose tissue may also introduce phase aberration and clutter into the ultrasound beams that are used to track the resultant displacements, compromising our ability to perform an accurate shear wave velocity reconstruction [15]. These sources of error and limitations will be addressed in future technical studies. Although the trend of decreasing successful stiffness reconstruction yield with increasing BMI was observed (Fig. 5), successful shear stiffness reconstructions were still achieved in patients with BMIs ranging from 15.7 to 66.0 kg/m^2.

There are several considerations to optimize the likelihood of successful shear stiffness reconstruction in patients. Good coupling between the ultrasound transducer and the skin must be maintained to achieve adequate displacement magnitudes; poor coupling leads to a loss of acoustic energy at the skin interface, which exacerbates the challenge of generating adequate displacements in patients with high BMIs. The imager must also make sure that high-quality B-mode images are being made prior to data acquisition. Typically, the location where the needle biopsy was performed (intercostal) provided the best qualitative imaging ROI since it had the least subcutaneous adipose tissue in the acoustic propagation path compared with the other imaging locations. B-mode images should target a uniform region of liver parenchyma, as shown in Fig. 1, and be devoid of rib shadowing and liver substructures that can lead to data artifacts associated with poor SNR and shear wave interactions with these entities. Motion artifacts can present challenges in some study subjects. The most common sources of motion in these studies were cardiac motion (which can be excessive in subcostal imaging locations that approach the sternal notch) and poor patient compliance with suspending their breathing during data acquisition. Additionally, the operator must take care to maintain a steady hand while acquiring data.

This study demonstrates that shear stiffness reconstructions based on acoustic radiation force excitations can be used to non-invasively evaluate liver fibrosis in patients being evaluated for NAFLD, including those with high BMI and ascites. These shear stiffnesses can be directly related to the liver fibrosis stage without being confounded by the imaging location, hepatocyte ballooning, or hepatic inflammation.

Conflict of interest

The authors who have taken part in this study declared that they do not have anything to disclose regarding funding or conflict of interest with respect to this manuscript.

References

[1] Angulo P. Nonalcoholic fatty liver disease. N Engl J Med 2002;346: 1221–1231.

[2] Wieckowska A, Feldstein AE. Nonalcoholic fatty liver disease in the pediatric population: a review. Curr Opin Pediatr 2005;17:636–641.

[3] Szczepaniak LS, Nurenberg P, Leonard D, Browning JD, Reingold JS, Grundy S, et al. Magnetic resonance spectroscopy to measure hepatic triglyceride content: prevalence of hepatic steatosis in the general population. Am J Physiol Endocrinol Metab 2004;288:E462–E468.

[4] Brunt EM, Janney CG, Di Biceglie AM, Neuschwander-Tetri BA, Bacon BR. Nonalcoholic steatohepatitis: a proposal for grading and staging the histological lesions. Am J Gastroenterol 1999;94:2467–2474.

[5] Matteoni CA, Younossi ZM, Gramlich T, Liu Y, Rybicki L, McCullough AJ. Nonalcoholic fatty liver disease: risk factors and long-term outcomes for benign versus aggressive disease. Gastroenterology 1998;114: 1413–1419.

[6] Wieckowska A, Feldstein AE. Diagnosis of nonalcoholic fatty liver disease: invasive versus noninvasive. Semin Liver Dis 2008;28:386–395.

[7] Wieckowska A, McCullough AJ, Feldstein AE. Noninvasive diagnosis and monitoring of nonalcoholic steatohepatitis: present and future. Hepatology 2007;46:582–589.

[8] Ratziu V, Charlotte F, Heurtier A, Gombert S, Giral P, Bruckert E, et al. Sampling variability of liver biopsy in nonalcoholic fatty liver disease. Gastroenterology 2005;128:1898–1906.

[9] Takemoto R, Nakamuta M, Aoyagi Y, Tatsuya F, Yasutake K, Koga K, et al. Validity of FibroScan values for predicting hepatic fibrosis stage in patients with chronic HCV infection. J Diagn Dis 2009;10:145–148.

[10] Foucher J, Castera L, Berhard PH. Prevalence and factors associated with failure of liver stiffness measurement using FibroScan in a prospective study of 2114 examinations. Eur J Gastroenterol Hepatol 2006;18:411–412.

Genetic and Metabolic Diseases

Research Article

[11] Yoneda M, Yoneda M, Mawatari H, Fujita K, Endo H, Iida H, et al. Noninvasive assessment of liver fibrosis by measurement of stiffness in patients with nonalcoholic fatty liver disease (NAFLD). Dig Liver Dis 2008;40:371–378.

[12] Wong V, Vergnoil J, Wong G, Foucher J, Chan H, Le Bail B, et al. Diagnosis of fibrosis and cirrhosis using liver stiffness measurement in nonalcoholic fatty liver disease. Hepatology 2010;51:454–462.

[13] Yoneda M, Suzuki K, Kato S, Fujita K, Nozaki Y, Hosono K, et al. Nonalcoholic fatty liver disease: US-based acoustic radiation force impulse elastography. Radiology 2010;256:640–647.

[14] Sarvazyan A, Rudenko OV, Swanson SD, Fowlkes JB, Emelianov SY, et al. Shear wave elasticity imaging: a new ultrasonic technology of medical diagnostics. Ultrasound Med Biol 1998;24:1419–1435.

[15] Palmeri ML, Wang MH, Dahl JJ, Frinkley KD, Nightingale KR. Quantifying hepatic shear modulus in vivo using acoustic radiation force. Ultrasound Med Biol 2008;34:546–558.

[17] Bercoff J, Tanter M, Fink M. Supersonic shear imaging: a new technique for soft tissue elasticity mapping. IEEE Trans Ultrason Ferroelectr Freq Control 2004;51:396–409.

[18] Sandrin L, Tanter M, Gennisson J, Catheline S, Fink M. Shear elasticity probe for soft tissues with 1-D transient elastography. IEEE Trans Ultrason Ferroelectr Freq Control 2002;49:436–446.

[19] Wang M, Palmeri ML, Rotemberg VM, Rouze NC, Nightingale KR. Improving the robustness of time-of-flight based shear wave speed reconstruction methods using RANSAC in human liver in vivo. Ultrasound Med Biol 2010;36:802–813.

[20] Loaeza-del-Castillo A, Paz-Pineda F, Oviedo-Cardenas E, Sanchez-Avilia F, Vargas-Vorackova F. AST to platelet ratio index (APRI) for the noninvasive evaluation of liver fibrosis. Ann Hepatol 2008;7:350–357.

[21] Wai C, Greenson J, Fontana R, Kalbfleisch J, Marrero J, Conjeevaram H, et al. A simple noninvasive index can predict both significant fibrosis and cirrhosis in patients with chronic hepatitis C. Hepatology 2003;38:518–526.

[22] Kleiner DE, Brunt EM, Van Natta M, Behling C, Contos MJ, Cummings OW, et al. Design and validation of a histological scoring system for nonalcoholic fatty liver disease. Hepatology 2005;41:1313–1321.

[23] Millonig G, Friedrich S, Adolfl S, Fonouni H, Golriz M, Mehrabi A, et al. Liver stiffness is directly influenced by central venous pressure. J Hepatol 2010;52:206–210.

[24] Frulio N, Laumonier H, Balabaud C, Trillaud H, Bioulac-Sage P. Hepatic congestion plays a role in liver stiffness. Hepatology 2009;50:1674–1675.

[25] Rifai K, Bahr M, Maderacke I. Acoustic radiation force imaging (ARFI) as a new method of ultrasonographic elastography allows accurate and flexible assessment of liver stiffness. J Hepatol 2009;50:S88.

[26] Lupsor M, Badea R, Stefanescu H, Sparchez Z, Branda H, Serban A, et al. Performance of a new elastographic methods (ARFI technology) compared to unidimensional transient elastography in the noninvasive assessment of chronic hepatitis C. Preliminary results. J Gastrointest Liver Dis 2009;18:303–310.

[27] Friedrich-Rust M, Wunder K, Kriener S, Sotoudeh F, Richter S, Bojunga J, et al. Liver fibrosis in viral hepatitis: noninvasive assessment with acoustic radiation force impulse imaging versus transient elastography. Radiology 2009;252:595–604.

[28] Huwart L, Peeters F, Sinkus R, Annet L, Salameh N, ter Beek LC, et al. Liver Fibrosis: non-invasive assessment with MR elastography. NMR Biomed 2006;19:173–179.

[29] Rouviere O, Yin M, Dresner A, Rossman PJ, Burgart LJ, Fidler JL, et al. MR elastography of the liver: preliminary results. Radiology 2006;240:440–448.

[30] Bercoff J. ShearWave Elastography (White Paper). SuperSonic Imagine 2008.

[31] Muller M, Gennisson JL, Deffieux T, Tanter M, Fink M. Quantitative viscoelasticity mapping of human liver using supersonic shear imaging: preliminary in vivo feasibility study. Ultrasound Med Biol 2009;35:219–229.

[32] Sandrin L, Miette V. Vibration-controlled transient elastography VCTE™ (White Paper). EchoSens™; 2010.